View metadata, citation and similar papers at core.ac.uk
brought to you by CORE
provided by Wageningen University & Research Publica

GEOPHYSICAL RESEARCH LETTERS, VOL. 34, L17402, doi:10.1029/2007GL031001, 2007

Click Here for Full Article

Dry-end surface soil moisture variability during NAFE'06

A. J. Teuling,[1,2] R. Uijlenhoet,[1] R. Hurkmans,[1] O. Merlin,[3] R. Panciera,[3] J. P. Walker,[3] and P. A. Troch[4]

Received 23 June 2007; revised 19 July 2007; accepted 8 August 2007; published 13 September 2007.

[1] Characterization of the space-time variability of soil moisture is important for land surface and climate studies. Here we develop an analytical model to investigate how, at the dry-end of the soil moisture range, the main characteristics of the soil moisture field (spatial mean and variability, steady state distribution) depend on the intermittent character of low intensity rain storms. Our model is in good agreement with data from the recent National Airborne Field Experiment (NAFE'06) held in the semiarid Australian Murrumbidgee catchment. We find a positive linear relationship between mean soil moisture and its associated variability, and a strong dependency of the temporal soil moisture distribution to the amount and structure of precipitation. **Citation:** Teuling, A. J., R. Uijlenhoet, R. Hurkmans, O. Merlin, R. Panciera, J. P. Walker, and P. A. Troch (2007), Dry-end surface soil moisture variability during NAFE'06, *Geophys. Res. Lett.*, *34*, L17402, doi:10.1029/2007GL031001.

1. Introduction

[2] The central role of soil moisture in the climate system is nowadays widely recognized. Soil moisture directly controls the water- and energy budgets at the land surface, and may also affect the peristence of anomalous atmospheric conditions. Global soil moisture monitoring, however, is complicated due to large spatial and temporal variability of soil moisture. Passive microwave remote sensing is among the most promising techniques, but its applicability is complicated by its shallow sensing depth (few cm) and the coarse spatial resolution (tens of km) of space-borne sensors (such as the upcoming Soil Moisture and Ocean Salinity mission, SMOS). Methods to quantify the space-time dynamics of the surface soil moisture field can lead to improved sampling, retrieval, validation, and downscaling.

[3] Previous field experiments have shown that the spatial variability of surface soil moisture may depend, among other factors, on the spatial mean soil moisture state. *Reynolds* [1970] has already hypothesized that due to the effect of soil heterogeneity, spatial variability increases during infiltration, and is minimum after dry-down. Based on detailed observations along a hillslope transect, *Famiglietti et al.* [1998] found that the spatial mean and variance have identical behavior. Both peaked after rainfall events, and decreased rapidly during dry-down. While both studies reported a decrease in variability with decreasing spatial mean soil moisture, opposite or more complex relations have also been reported [e.g., *Teuling and Troch*, 2005; *Teuling et al.*, 2007]. A theoretical framework to analyze the changes in spatial variability of root-zone soil moisture was presented by *Albertson and Montaldo* [2003]. Here we apply this framework to study surface layer soil moisture in the dry-end of the soil moisture range. The model is a limited case of the more comprehensive models utilized by *Albertson and Montaldo* [2003] and *Teuling and Troch* [2005], and allows for full analytical characterization of the spatial and temporal soil moisture variability. The model is subsequently tested on a unique, recently collected data set.

2. Data

[4] The 3-week long National Airborne Field Experiment 2006 (NAFE'06) was undertaken in the Australian Murrumbidgee catchment (Figure 1A) during October–November 2006. The region experienced severe drought conditions from 2001 onwards, and had no rainfall in the five weeks preceding the campaign. In the Murray Darling basin, 2006 was the third driest year on record. Fortunately, during NAFE'06 there were several minor rainfall events totaling ~20 mm (Table 1, Figure 2A). The objective of NAFE'06 was to provide data for SMOS soil moisture retrieval, downscaling, and data assimilation (see http://www.nafe.unimelb.edu.au). Ground observations of surface soil moisture were made at 6 field sites in the 60 × 60 km Yanco region (35°S, 146°E, Figure 1B). At each field, point soil moisture and precipitation were recorded at 20 min resolution. Here we analyse soil moisture variability in the non-irrigated fields Y2, Y7, and Y10, which are all dry pastures used for grazing. The predominant soil type is clay.

[5] Soil moisture observations were made by means of the Hydraprobe Data Acquisition System [HDAS, *Panciera et al.*, 2006], which integrates a GPS and the Vitel Hydra Probe® [*Seyfried and Murdock*, 2004] in a GIS environment. (The mention of product names does not constitute an endorsement of this product.) HDAS made it possible to rapidly monitor surface (0–5 cm) soil moisture on a predefined grid within large field sites. During NAFE'06, the different teams took a total of 16,937 HDAS readings. A maximum number of 3 separate readings were taken at each sampling location in order to get a representative point-scale value. HDAS observations were calibrated against gravimetric measurements (taken

[1]Hydrology and Quantitative Water Management Group, Wageningen University, Wageningen, Netherlands.
[2]Now at Institute for Atmospheric and Climate Science, ETH Zürich, Zürich, Switzerland.
[3]Department of Civil and Environmental Engineering, The University of Melbourne, Melbourne, Australia.
[4]Department of Hydrology and Water Resources, The University of Arizona, Tucson, Arizona, USA.

Copyright 2007 by the American Geophysical Union.
0094-8276/07/2007GL031001$05.00

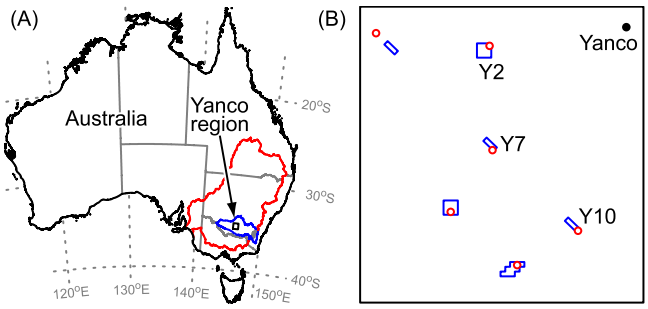

Figure 1. Map of the Yanco region. (A) Location within the Murray Darling basin (red) and the Murrumbidgee catchment (blue). (B) Location of the NAFE'06 field sites (blue) and rainfall stations (○).

throughout the campaign at different locations) by means of a third-order polynomial regression. Some field-scale statistics are summarized in Table 1.

3. Temporal Dynamics

[6] In developing our model, we consider the volumetric soil moisture θ in a shallow surface layer of depth L. In dry conditions, this layer is effectively "decoupled" from the deeper soil moisture [*Capehart and Carlson*, 1997]. For convenience, we only model the dynamics of the transformed soil moisture $\vartheta = \theta - \xi$, where ξ is the residual soil moisture content. In the following, we denote the field-scale mean of any quantity x by $\overline{x}$, and its standard deviation by σ_x. With little vegetation and low intensity rainfall, the water balance is dominated by infiltration of precipitation (P) and evaporation. Both processes occur in an alternating fashion, with the latter process being much slower.

[7] During storms ($P > 0$), point-scale variability in land surface properties (e.g., texture, vegetation, micro-topography, macropores) causes variable infiltration [e.g., *Reynolds*, 1970]. Without explicitely modeling these processes, we assume that at any point a fixed fraction (α) of P contributes to the antecedent soil moisture. During interstorm periods ($P = 0$), daily evaporation is proportional to the available surface moisture ϑ [*Kurc and Small*, 2004]. The resulting point-scale water balance is:

$$\frac{\mathrm{d}\vartheta}{\mathrm{d}t} = \begin{cases} \alpha P/L, & P > 0 \\ -\vartheta/\tau, & P = 0, \end{cases} \tag{1}$$

where τ is the time scale of surface evaporation. In practice, τ will also be subject to spatial variability. In the model however, a spatial variability in τ introduces a complicating time-dependent covariance between α and ϑ, which would also destroy rank stability (see below). Since drydown is a dissipative process, this simplification has little impact on the results. The horizontal average of (1) at the field-scale ($\sim$1 km^2) is obtained by replacing ϑ and α by their field-scale means $\overline{\vartheta}$ and $\overline{\alpha}$, respectively:

$$\frac{\mathrm{d}\overline{\vartheta}}{\mathrm{d}t} = \begin{cases} \overline{\alpha} P/L, & P > 0 \\ -\overline{\vartheta}/\tau, & P = 0, \end{cases} \tag{2}$$

where spatial variability of P at the field-scale is neglected. Integrating (2) over different periods with constant P, each starting at subsequent t_0 and of duration Δt, yields:

$$\overline{\vartheta}(t_0 + \Delta t) = \begin{cases} \overline{\vartheta}(t_0) + \overline{\alpha}\frac{P}{L}\Delta t, & P > 0 \\ \overline{\vartheta}(t_0) e^{-\Delta t/\tau}, & P = 0. \end{cases} \tag{3}$$

[8] The simplified water balance can also be written in terms of its deviations (ϑ') from the spatial mean (i.e., $\vartheta' =$

Table 1. Regional precipitation P, and mean ($\overline{\theta}$) and standard deviation (σ_θ) of the field-scale soil moisture surveys

		Y2[a]		Y7[b]		Y10[b]	
DOY	P, mm	$\overline{\theta}$	σ_θ	$\overline{\theta}$	σ_θ	$\overline{\theta}$	σ_θ
304	0.0	0.0319	0.0166	-	-	-	-
305	0.0	-	-	0.0310	0.0154	0.0218	0.0107
306	0.0	0.0319	0.0169	-	-	-	-
307	5.7	-	-	0.0801	0.0213	0.0763	0.0237
308	0.1	0.0578	0.0240	-	-	-	-
309	0.0	0.0400	0.0190	-	-	-	-
310	0.0	-	-	-	-	-	-
311	0.0	0.0315	0.0162	-	-	-	-
312	0.0	-	-	0.0320	0.0146	0.0245	0.0135
313	0.0	0.0294	0.0157	-	-	-	-
314	0.0	-	-	0.0312	0.0146	0.0262	0.0138
315	0.0	-	-	-	-	-	-
316	0.0	-	-	-	-	-	-
317	2.1	0.1592	0.0444	-	-	-	-
318	11.3	0.1151	0.0426	-	-	-	-
319	0.0	-	-	0.0800	0.0275	0.0828	0.0284
320	1.0	0.0849	0.0234	-	-	-	-
321	0.0	-	-	0.0741	0.0253	0.0654	0.0310
322	0.0	0.0683	0.0249	-	-	-	-

[a]Regular 12 × 12 grid, 250 m spacing (3 × 3 km^2).
[b]Regular 46 × 5 grid, 50 m spacing (2.3 × 0.25 km^2).

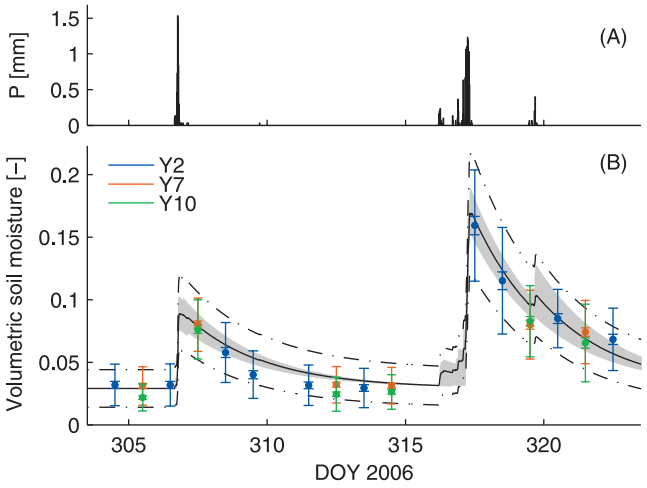

Figure 2. Precipitation and soil moisture during NAFE'06. (A) Regional average precipitation (20 min). (B) Soil moisture dynamics. Points are observed field-scale means, inner bounds the 95% confidence bounds for $\overline{\theta}$, and outer bounds $\overline{\theta} \pm \sigma_\theta$. Solid line is simulated $\overline{\theta}$ with (3) forced with regional average P, dash-dotted lines are $\overline{\theta} \pm \sigma_\theta$ with (5). Grey area markes the range in $\overline{\theta}$ in response to regional-scale variability in P.

$\vartheta - \overline{\vartheta}$). Multiplying the resulting equation by $2\vartheta'$, applying the chain rule ($2\vartheta' \mathrm{d}\vartheta'/\mathrm{d}t = \mathrm{d}\vartheta'^2/\mathrm{d}t$), and spatially averaging the result yields the spatial variance budget *Albertson and Montaldo* [2003]:

$$\frac{\mathrm{d}\overline{\vartheta'^2}}{\mathrm{d}t} = \frac{\mathrm{d}\sigma_\vartheta^2}{\mathrm{d}t} = \begin{cases} \frac{2P}{L}\overline{\alpha'\vartheta'}, & P > 0 \\ -\frac{2}{\tau}\sigma_\vartheta^2, & P = 0, \end{cases} \tag{4}$$

where $\overline{\alpha'\vartheta'}$ is the covariance between α and ϑ. By using $\overline{\alpha'\vartheta'} = \sigma_\alpha \sigma_\vartheta \rho_{\alpha,\vartheta}$, where $\rho_{\alpha,\vartheta}$ is the correlation coefficient between α and ϑ, and the chain rule ($\mathrm{d}\sigma_\vartheta^2/\mathrm{d}t = 2\sigma_\vartheta \mathrm{d}\sigma_\vartheta/\mathrm{d}t$), (4) can be further simplified. In this case, ϑ' is linearly (and only) related to α', so $\rho_{\alpha,\vartheta} = 1$. Time integration yields:

$$\sigma_\vartheta(t_0 + \Delta t) = \begin{cases} \sigma_\vartheta(t_0) + \sigma_\alpha \frac{P}{L}\Delta t, & P > 0 \\ \sigma_\vartheta(t_0) e^{-\Delta t/\tau}, & P = 0, \end{cases} \tag{5}$$

which, due to the linear character of the model, is functionally equivalent to (3). For simplicity, we also assume $\rho_{\alpha,\xi} = 1$, so that $\sigma_\theta = \sigma_\vartheta + \sigma_\xi$. Through our formulation we ensure perfect rank stability of point-scale soil moisture (i.e., temporal persistence in the spatial pattern), which is required in order not to violate the assumption that $\rho_{\alpha,\vartheta} = 1$. The existence of rank (or time) stability in surface soil moisture fields was shown by *Jacobs et al.* [2004]. Since changes in $\overline{\theta}$ and σ_θ in (3) and (5), respectively, are both proportional to P, the relation between $\overline{\theta}$ and σ_θ is linear:

$$\sigma_\theta(\overline{\theta}) = CV_\alpha(\overline{\theta} - \overline{\xi}) + \sigma_\xi, \qquad \overline{\theta} \geq \overline{\xi}. \tag{6}$$

where $CV_\alpha = \sigma_\alpha/\overline{\alpha}$ is the coefficient of variation of α.

[9] The parameter values are given in Table 2. First, $\overline{\xi}$ was taken as the average observed values of $\overline{\theta}$ before the first rainfall (here DOY 306). τ was taken from *Kurc and Small* [2004], and $\overline{\alpha}$ was optimized such that the amplitude of $\overline{\theta}$ was in correspondence with the observations. Next, σ_α and σ_ξ were adjusted such that (6) corresponds to the linear regression $\sigma_\theta = a\overline{\theta} + b$ between all observed $\overline{\theta}$ and σ_θ ($\sigma_\alpha = a\overline{\alpha}$ and $\sigma_\xi = b + \overline{\xi}\sigma_\alpha/\overline{\alpha}$). Initial conditions for $\overline{\vartheta}$ and σ_ϑ are $\overline{\xi}$ and σ_ξ, respectively. We use $\Delta t = 20$ min.

[10] The simultaneous increase of $\overline{\theta}$ and σ_θ during storms of low intensity, and their subsequent decrease during interstorm periods, is apparent in both the simulations and observations (Figure 2B). The decay timescale of *Kurc and Small* [2004] works well for the NAFE'06 conditions, with the observed amplitude and dynamics of $\overline{\theta}$ and σ_θ captured by the model. Regional scale precipitation variability induces only small variability in the field-scale responses of $\overline{\theta}$, which is also suggested by the similar pattern of observed $\overline{\theta}$ and σ_θ. The changes in top 5 cm soil moisture were found to account for over half of the precipitation ($\overline{\alpha} = 0.53$).

4. Mean Versus Variability

[11] The relation between the spatial mean and variability is of interest for scaling. The modeled relation between $\overline{\theta}$ and σ_θ is given by (6). Note that (6) is independent of the interstorm decay time τ. Recently, *Choi et al.* [2007] investigated the relation between the spatial mean soil moisture and coefficient of variation (CV_θ) for a number of datasets. They optimized the parameters A and B in the empirical model $CV_\theta(\overline{\theta}) = A \exp(B\overline{\theta})$. Here, this relation is hyperbolic:

$$CV_\theta(\overline{\theta}) = CV_\alpha + \frac{1}{\overline{\theta}}(\sigma_\xi - \overline{\xi} CV_\alpha), \qquad \overline{\theta} \geq \overline{\xi}. \tag{7}$$

[12] Figure 3 shows the observed and simulated relation between $\overline{\theta}$ and σ_θ. Overall, the (linear) model explains 88% of the variance in all observed σ_θ. Separate analysis of Y2, Y7, and Y10, yields R^2 values of 0.92, 0.86, and 0.83, respectively. The regressions are similar for all sites, confirming the validity of our assumption that the field-scale soil moisture within the region responds similarly to a given precipitation input.

[13] The relative variability CV_θ decreases with increasing $\overline{\theta}$ (Figure 3). Since the absolute variability increases with $\overline{\theta}$, the decrease of CV_θ can be attributed to the increase in $\overline{\theta}$. For the exponential *Choi et al.* model, we find parameters $A =$

Table 2. Parameters and their values

Parameter	Symbol	Value	Units
Surface layer depth	L	50.0	mm
Infiltration fraction (mean)	$\overline{\alpha}$	0.53	-
Infiltration fraction (sd)	σ_α	0.13	-
Evaporation decay time	τ	2.8[a]	d
Residual moisture content (mean)	$\overline{\xi}$	0.029	-
Residual moisture content (sd)	σ_ξ	0.015	-
Mean storm depth	η	2.1	mm
Mean storm arrival rate	λ	0.50	d^{-1}

[a]Taken from *Kurc and Small* [2004] for semiarid grassland.

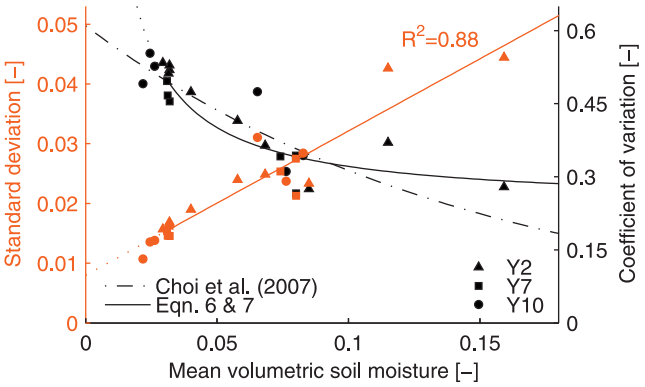

Figure 3. Relation between field-scale spatial mean and spatial variability of surface soil moisture.

0.61 and $B = -0.067$ [with soil moisture expressed in % as in *Choi et al.*, 2007]. The difference between the models increases for $\overline{\theta} > 0.10$, partly due to the different fitting procedures (i.e., fitting CV_θ or σ_θ). Although there is an obvious physical limit to the increase of σ_θ with $\overline{\theta}$ due to the presence of the upper bound at porosity, this limit was not reached during NAFE'06. The added value of our model (7) with respect to the *Choi et al.* model lies in the fact that it can be interpreted in terms of the underlying processes.

5. Steady State Distribution

[14] The dynamics of soil moisture is governed by the occurence and amount of rainfall (Figure 2), which are both stochastic. We investigate the impact of climate variability (through P) on the steady-state soil moisture distribution $f(\overline{\vartheta})$ (or $f(\vartheta)$) by including a stochastic representation of rainfall pulses in the model. Here, storms occur instantaneously, and can be described by a marked Poisson process. The depth of storm events and the interarrival times are considered independent random variables. Both are exponentially distributed with mean η and λ^{-1}, respectively. The mean rain rate $\langle P \rangle$ equals $\eta\lambda$. We estimate λ from the (spatial) average number of non-interrupted rainless sequences during NAFE'06 at the 20 min resolution, and η from the corresponding total rainfall over the same period (Table 2). In this simplified case, the resulting steady-state distribution is a shifted Gamma pdf (Appendix A):

$$f(\overline{\vartheta}) = \frac{(\overline{\vartheta})^{\lambda\tau-1}\exp(-c\overline{\vartheta})}{c^{-\lambda\tau}\Gamma(\lambda\tau)}, \qquad (8)$$

where $c = (\overline{\alpha}\eta/L)^{-1}$. This distribution has mean $\overline{\xi} + \lambda\tau c^{-1}$ and standard deviation $(\lambda\tau)^{1/2}c^{-1}$. For $\lambda\tau = 1$, (8) reduces to a shifted exponential distribution. Although (8) is written in terms of field-scale averages, it is equally valid at the point-scale by using the appropriate α. Figure 4 shows the resulting $f(\overline{\theta})$ and its sensitivity to climate scenarios. In the wet scenario ($\langle P \rangle^+$), $\langle P \rangle$ is doubled either by an increase in η or λ (η^+ and λ^+, respectively). Similarly, we assume $\langle P \rangle$ to be halved in the dry scenario ($\langle P \rangle^-$).

[15] For the NAFE'06 conditions, which were below the climatic average, the mean and standard deviation of the steady-state soil moisture distribution are 0.061 and 0.027, respectively. Its distribution is unimodal and positively skewed. The positive skew is due to the decreasing evaporation towards $\overline{\xi}$, corresponding to smaller $d\overline{\vartheta}/dt$, and subsequently larger $f(\overline{\vartheta})$. Independent high resolution point-scale observations at Y10 (Figure 4) confirm the validity of the model. Their distribution is also unimodal and positively skewed, with mean 0.064 and standard deviation 0.028. The wet scenario $\langle P \rangle^+$ results in a mean soil moisture of 0.093, the dry scenario $\langle P \rangle^-$ in 0.045. While the mean soil moisture depends on $\langle P \rangle$ and not on its temporal structure (i.e., on the balance between η and λ), this structure does influence the steady state variability. When changes in $\langle P \rangle$ are caused by changes in mean storm depth η (i.e., η^+ and η^-), the temporal variability is largest. Since the temporal standard deviation is proportional to η, it is twice as high under η^+ than under NAFE'06 conditions (0.054 and 0.027, respectively). A reduction in mean storm frequency (λ^-) causes a shift in the mode of $f(\overline{\theta})$ towards $\overline{\xi}$.

6. Discussion and Conclusion

[16] An analytical model to study daily surface soil moisture variability dynamics in the dry-end of the soil moisture range has been developed. Under the low intensity rainfall encountered during NAFE'06, the dynamics of soil moisture are well reproduced by using a linear relationship between soil moisture and daily evaporation. We found that the spatial mean and standard deviation rapidly increased during rainfall, and slowly decreased during interstorm periods. The temporal distribution of surface soil moisture was found to be highly sensitive to the amount and structure of precipitation. The results are consistent with previous experiments [*Kurc and Small*, 2004; *Reynolds*, 1970; *Famiglietti et al.*, 1998], and allow for a more quantitative (water balance-based) approach to surface soil moisture variability. More comprehensive models, for instance those utilized by *Albertson and Montaldo* [2003]

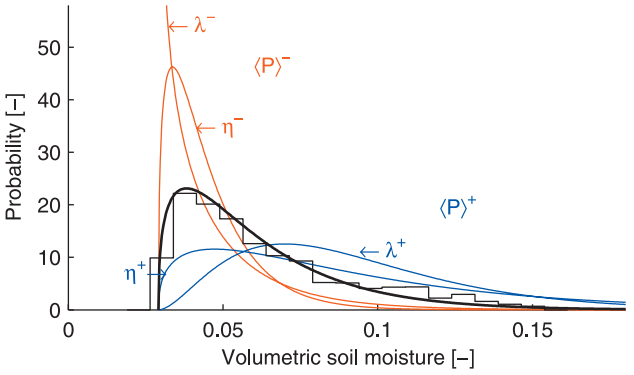

Figure 4. Steady-state distribution of field-scale mean soil moisture during NAFE'06 and its sensitivity to precipitation characteristics. Histogram shows the distribution of 20 min resolution point-scale soil moisture (0–5 cm) at Y10 for DOY 298–327.

and *Teuling and Troch* [2005], are valid at the full soil moisture range, but require numerical solution.

Appendix A: Derivation of $f(\overline{\theta})$

[17] Let an instantaneous rainfall event contribute an exponentially distributed amount I with mean μ ($= c^{-1}$) to transformed soil moisture ϑ. Furthermore, let ϑ_- be the value of ϑ immediately preceding, and ϑ_+ directly after the event ($\vartheta_+ = \vartheta_- + I$). In the steady state, the pdf of ϑ_- ($f_{\vartheta_-}(\vartheta)$) equals the pdf of soil moisture at the end of the drydown following the event. In addition, if rainfall occurrence follows a Poisson process, then $f_{\vartheta}(\vartheta)$ equals $f_{\vartheta_-}(\vartheta)$.

[18] We have to show that:

$$f_{\vartheta_-}(\vartheta) = \frac{\vartheta^{\lambda\tau-1}\exp\left(-\frac{\vartheta}{\mu}\right)}{\mu^{\lambda\tau}\Gamma(\lambda\tau)}, \tag{A1}$$

is the steady state pdf of ϑ. Because soil moisture decays exponentially (with constant τ) during drydown, and the duration of drydown periods follows an exponential pdf with mean $1/\lambda$, the conditional pdf $f_{\vartheta_-|\vartheta_+}(\vartheta)$ is:

$$f_{\vartheta_-|\vartheta_+}(\vartheta) = \frac{\lambda\tau}{\vartheta}\left(\frac{\vartheta}{\vartheta_+}\right)^{\lambda\tau}. \tag{A2}$$

Hence the unconditional pdf of ϑ_- becomes:

$$f_{\vartheta_-}(\vartheta) = \int_{\vartheta}^{\infty} f_{\vartheta_-|\vartheta_+}(\vartheta) f_{\vartheta_+}(\vartheta_+)\mathrm{d}\vartheta_+. \tag{A3}$$

Because ϑ_- and I are independent random variables, $f_{\vartheta_+}(\vartheta)$ is the convolution of $f_I(I)$ and $f_{\vartheta_-}(\vartheta)$:

$$f_{\vartheta_+}(\vartheta) = \frac{1}{\mu}\int_0^{\vartheta} \exp\left(-\frac{\vartheta - I}{\mu}\right) f_{\vartheta_-}(I)\mathrm{d}I \tag{A4}$$

Substituting (A1) in (A4) leads to $f_{\vartheta_+}(\vartheta)$. Subsequently substituting this result in (A3) again produces (A1).

[19] **Acknowledgments.** We thank the NAFE'06 team for their efforts in collecting the soil moisture data. This research was supported by the Australian Research Council (Project DP0557543), the Wageningen Institute for Environment and Climate Research (WIMEK), the Research programme Climate Change of Wageningen University and Research Center, and the project Development of a European Land Data Assimilation System to predict Floods and Droughts (ELDAS, EVG1-CT-2001-00050). A.J.T. and R.H. acknowledge support from the Netherlands Organisation for Scientific Research (NWO) through Travel Grants R84-630 and R84-631. R.U. acknowledges financial support from NWO through a Innovational Research Incentives Scheme grant (Project 016.021.003).

References

Albertson, J. D., and N. Montaldo (2003), Temporal dynamics of soil moisture variability: 1. Theoretical basis, *Water Resour. Res.*, *39*(10), 1274, doi:10.1029/2002WR001616.

Capehart, W. J., and T. N. Carlson (1997), Decoupling of surface and near-surface soil water content: A remote sensing perspective, *Water Resour. Res.*, *33*(6), 1383–1395.

Choi, M., J. M. Jacobs, and M. Cosh (2007), Scaled spatial variability of soil moisture fields, *Geophys. Res. Lett.*, *34*(1), L01401, doi:10.1029/2006GL028247.

Famiglietti, J. S., J. W. Rudnicki, and M. Rodell (1998), Variability in surface moisture content along a hillslope transect: Rattlesnake Hill, Texas, *J. Hydrol.*, *210*, 259–281.

Jacobs, J. M., B. P. Mohanty, E. Hsu, and D. Miller (2004), SMEX02: Field scale variability, time stability and similarity of soil moisture, *Remote Sens. Environ.*, *92*, 436–446, doi:10.1016/j.rse.2004.02.017.

Kurc, S. A., and E. E. Small (2004), Dynamics of evapotranspiration in semiarid grassland and schrubland ecosystems during the summer monsoon season, central New Mexico, *Water Resour. Res.*, *40*, W09305, doi:10.1029/2004WR003068.

Panciera, R., O. Merlin, R. Young, and J. Walker (2006), *The Hydraprobe Data Acquisition System: User guide*, Department of Civil and Environmental Engineering, The University of Melbourne.

Reynolds, S. G. (1970), The gravimetric method of soil moisture determination, Part III, An examination of factors influencing soil moisture variability, *J. Hydrol.*, *11*(3), 288–300.

Seyfried, M. S., and M. D. Murdock (2004), Measurement of soil water content with a 50-MHz soil dielectric sensor, *Soil Sci. Soc. Am. J.*, *68*, 394–403.

Teuling, A. J., and P. A. Troch (2005), Improved understanding of soil moisture variability dynamics, *Geophys. Res. Lett.*, *32*(5), L05404, doi:10.1029/2004GL021935.

Teuling, A. J., F. Hupet, R. Uijlenhoet, and P. A. Troch (2007), Climate variability effects on spatial soil moisture dynamics, *Geophys. Res. Lett.*, *34*(6), L06406, doi:10.1029/2006GL029080.

R. Hurkmans and R. Uijlenhoet, Hydrology and Quantitative Water Management Group, Wageningen University, Droevendaalsesteeg 4, Atlas Building (104), P. O. Box 47, NL-6700 AA, Wageningen, Netherlands.

O. Merlin, R. Panciera, and J. P. Walker, Department of Civil and Environmental Engineering, University of Melbourne, Parkville, Vic, 3010, Australia.

A. J. Teuling, Institute for Atmospheric and Climate Science, ETH Zürich, CHN M 17.2, Universitätstrasse 16, CH-8092 Zürich, Switzerland. (ryan.teuling@env.ethz.ch)

P. A. Troch, Department of Hydrology and Water Resources, The University of Arizona, P. O. Box 210011, Tucson, AZ 85721, USA.